applied sciences

MDPI

Article

Improving the Structural Behavior of Tied-Arch Bridges by Doubling the Set of Hangers

Juan Manuel García-Guerrero * and Juan José Jorquera-Lucerga

Mining and Civil Engineering Department, Universidad Politécnica de Cartagena (UPCT), Paseo Alfonso XIII, 50, 30203 Cartagena, Spain; juanjo.jorquera@upct.es

* Correspondence: jm.guerrero@upct.es

Received: 14 October 2020; Accepted: 3 December 2020; Published: 4 December 2020

Featured Application: The conclusions of this paper could be useful for practicing structural engineers, mainly in the first stages of the conceptual design of arch bridges.

Abstract: In tied-arch bridges with a single arch, the deck is usually suspended from the arch by means of a single set of cables, pinned at both ends and anchored to the centerline, using either vertical or Nielsen-type hanger arrangements. When properly designed, this layout can significantly reduce forces and deflections under loads that are symmetrical with respect to the plane of the arch. However, it does not contribute to the support of nonsymmetrical loads, such as eccentric loads distributions or wind loading, and does not reduce the sensibility of the arch to out-of-plane buckling. Thus, this paper studies how a cable arrangement composed of two sets of lateral hangers, attached to both edges of a deck, can be very suitable to address these problems. Firstly, it is demonstrated that the structural behavior under symmetrical loads improves with respect to the bridge with centered hangers. Secondly, it is shown how nonsymmetric loads are partially carried by structural systems (such as the transversal stiffness both of the arch and the deck) that would remain inactive for tied-arch bridges with centered hangers, leading to a general reduction in the forces and the deflections of the bridge and in the critical buckling load of the arch.

Keywords: tied-arch bridge; conceptual design; preliminary design; hanger arrangement; buckling

1. Introduction

In tied-arch bridges with a single arch, the most common method of linking the arch and the deck is by suspending the deck from the arch by means of a single set of cables, pinned at both ends, anchored to the centerline. This configuration, when properly designed, can successfully help to meet the strength and stiffness requirements of a bridge, provided that the acting live loads are transversally symmetric, i.e., when the resultant live loads are contained within the plane of the arch, as described by Karnowsky [1] or Stavridis [2]. For example, in addition to the classical vertical hangers arrangement (Figure 1a), the arch and the deck can be connected by means of a Nielsen-type arrangement (with V-shaped cables, resembling the diagonals of a truss), which, as it is known (García-Guerrero [3]), significantly reduces both deflections and forces within the vertical plane (Figure 1b). Further reductions of the arch's bending moments in the vertical plane can be obtained by refining the arch elevation so that it is as close as possible to the antifunicular geometry, as described by Jorquera-Lucerga [4].

However, the cable arrangement contained within a central vertical plane has virtually no capacity to help the bridge meet certain serviceability or failure criteria under nonsymmetric loads. i.e., not contained within the plane of the arch, such as eccentric live loads, wind loads (Thalla [5]), or dynamic and seismic loadings, as described by Gentile et al. [6] or Gou et al. [7]. This happens, for example, for vertical deflections

at the edge of the deck or out-of-plane buckling of the arch, as shown by Manterola-Armisén [8] and Palkowski [9] and detailed in Section 7.

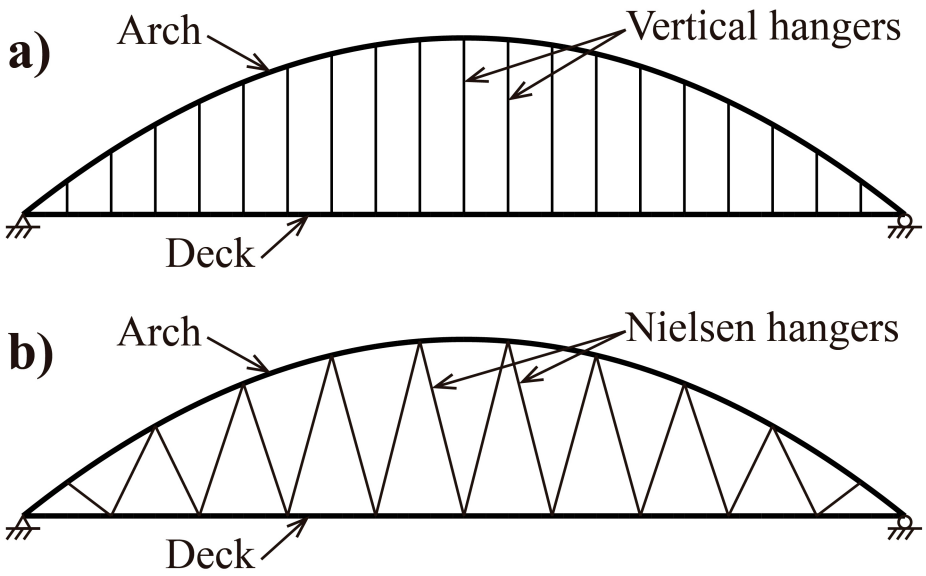

Figure 1. (**a**) Vertical and (**b**) Nielsen hanger arrangements.

Of course, these problems can be solved by increasing the size of the arch or the deck, as studied by García-Guerrero [3]. If the deck has a hollow-box cross-section, which is very common in bridges with a central hanger arrangement, the torsional stiffness can be increased by enlarging the area enclosed by the median line (i.e., its size). However, this is not always possible, e.g., due to clearance restrictions under the deck. Alternatively, the torsional stiffness of the cross-section can be increased by using thicker steel plates at the perimeter of the cross-section. Whatever the solution, it implies an increase in the cost of the bridge. The cost increase can be very high since resisting equilibrium torsion is extremely expensive, as it happens in some bridges designed by Santiago Calatrava, where the equilibrium torsion is resisted by an eccentric torsion bar located at one edge of the deck, such as in the La Devesa footbridge (see Tzonis [10] and Jorquera-Lucerga [11]).

Another and more drastic approach to these problems is by duplicating the arches and placing each arch on an edge of the deck, a solution which also implies a significant increase in cost and, in addition, leads to a substantial alteration of both the structural behavior and the aesthetic appearance of the bridge. Another possible strategy is to use stiffened hangers, such as those shown in the bridge in Figure 2, which have the capacity to support shear and bending forces in addition to axial forces. This solution has been studied in detail by García-Guerrero and Jorquera-Lucerga [12,13] and involves additional structural systems (such as out-of-plane bending and torsional stiffness both of the arch and the deck) to help limit forces and deflections.

Finally, another possible alternative within the designer's possibilities, consists, simply, of doubling the set of hangers and attaching the arch to both edges of the deck (Figure 3b) by means of two lateral sets of hangers. This strategy is the focus of the research shown in this paper.

Thus, the objective of this paper is to study how a cable arrangement, composed of two sets of lateral hangers, that links the arch to the two edges of the deck can be used by the designer as a strategy to satisfy serviceability and failure requirements in a tied-arch bridge under eccentric loads, i.e., whose resultant is not contained in the plane of the arch. When properly used, this strategy has the advantage where the cross-sections, both of the arch and the deck, do not need to be enlarged. In fact, they can often be lightened, as will be shown in Section 4. Furthermore, it is shown how this cable arrangement does not worsen the structural behavior of the bridge in the vertical plane under symmetric loads with respect to those of bridges with a single centered set of hangers, and it will be

seen how, in the studied cases, the structural behavior improves. With the purpose of studying the advantages of this type of cable arrangement, the structural behavior of a series of tied-arch bridges has been studied both with vertical and Nielsen hangers and for bridges with one set of central hangers attached to the centerline of the deck (Figure 3a) and for two sets of lateral hangers anchored to its edges (Figure 3b). In Figure 3, f corresponds to the maximum vertical separation between the arch and the deck, i.e., the rise of the arch.

Figure 2. Tied-arch bridge in Tartu over the Emajõgi river (Estonia). Photo: HendrixEesti, Wikimedia Commons.

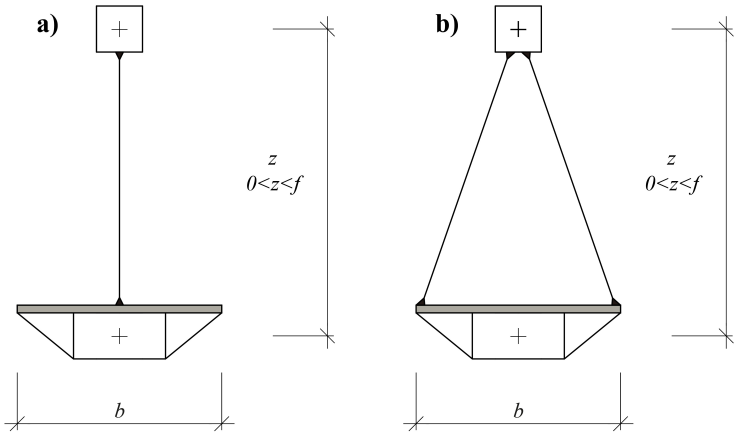

Figure 3. (**a**) One set of central hangers attached to the centerline of the deck. (**b**) Two sets of lateral hangers attached to the edges of the deck.

This paper begins by defining, in Section 2, the so-called reference models, which are two common bridge configurations (two tied-arch bridges, one with vertical hangers and the other with a Nielsen-type arrangement) on which all the bridges shown in this paper are based. Section 3 studies the behavior, in the vertical plane, of bridges with a single set of hangers under symmetric loads. The results of this section are compared with the results of the studies carried out in Section 3, Section 4, Section 5, Section 6, Section 7. In addition, it is shown how the cables anchored to the axis of the deck are not able to reduce the deflections due to the torsional twist of the deck. Section 4 introduces bridges that differ from those studied in Section 3 in that they have two sets of hangers attached to the edges of the deck. Their deflections and forces are studied. It is shown not only that their structural

behavior improves under eccentric loads but also that the behavior for symmetric loads improves with respect to that of the bridges with one central cable arrangement. Based on the results obtained in Section 4, Section 5 identifies the structural systems that support symmetric and nonsymmetric loads, i.e., actions contained within the plane of the arch and out-of-plane actions. The effect of the second set of hangers in the vertical response of the bridges will be discussed. In addition, it will be seen how some structural systems, such as the transversal and torsional stiffness both of the arch and the deck, become active under out-of-plane loads when the arch is linked with two sets of hangers to the deck. Section 6 shows how, in Nielsen-type bridges, due to nonsymmetric loads, the end hangers can be put into compression and loosen and how this problem can be solved by forking the ends of the arch. Section 7 discusses the buckling of this type of structure and shows how attaching the arch to both edges improves the out-of-plane buckling resistance of the arch. Furthermore, it is shown how forking the ends of the arch, as it happens, for example, in the Wittenberg Bridge (Figure 4), may also be a solution to improve the buckling resistance of the arch since its buckling length is reduced. The paper ends with the Conclusions section (Section 8).

Figure 4. Wittenberg Bridge over the Elbe River. Left: Forked railway tied-arch bridge with two sets of lateral hangers. Right: Road bridge with single central set of hangers. Photo: Michael Fiegle. Wikimedia Commons.

2. Reference Bridges and Considered Load Cases

The bridges shown in this paper are based on the reference bridges shown in Figure 5. As mentioned above, not only has a vertical center cable arrangement been considered but also a Nielsen-type layout (with inclined V-shaped hangers, such as the diagonal members of a curved-upper-chord truss, Figure 5b) because of its known effectiveness in reducing deflections and forces in classical vertical planar tied-arch bridges with one central set of hangers. The reference models have a span L = 100 m and a rise f = 20 m. The spacing between anchorages of the hangers in the deck is s = 5 m and s = 10 m for V1 and N1, respectively. The loaded width of the deck is b = 8 m. The bridge is assumed to have a relatively common configuration and, therefore, the cross-section of the arch is assumed to be an all-steel hollow-box section, whereas the cross-section of the deck is assumed to be a composite steel–concrete section composed of a steel box section and a reinforced concrete slab. Each end of the arch is fully fixed to the deck. The box has also transversal ribs, although they have no influence on

the global structural behavior. The self-weight of the concrete slab has been considered as part of the permanent loads, and the mechanical properties of the cross-section of the deck are, in a simplified way, assumed to be those of the hollow all-steel box cross-section described in Table 1. These dimensions are inspired by real arch bridges and are relatively common (see for example Leonhardt [14] or Lebet and Hirt [15]). All the bridges studied have been preliminarily designed according to Eurocode 3-2 [16]. The dimensions are shown in Table 1.

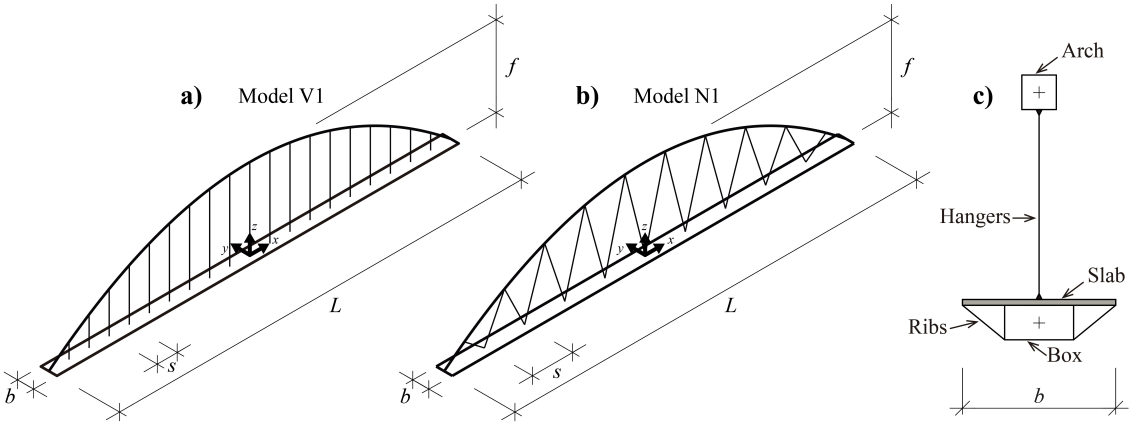

Figure 5. Reference models for a central set of hangers attached to the centerline of the deck: (**a**) vertical hangers; (**b**) Nielsen-type hangers; (**c**) cross-section.

Table 1. Definition of reference models.

Structural Element	Cross-Sections	Size [1]	Young's Modulus (N/mm^2)
Arch	Square hollow-box	1250 × 1250 mm, $t_f = t_w$ = 30 mm	2.0×10^5
Hangers	Solid circular	Ø 80 mm	1.6×10^5
Deck	Rectangular hollow-box	5000 × 1000 mm, $t_f = t_w$ = 20 mm	2.0×10^5

[1] t_f, t_w: thickness, respectively, of flanges and webs.

In the studied bridges, the stiffness of the cross-section of the hangers is a more restrictive criterion than the failure and serviceability checking. Therefore, the same cross-section has been used for all the hangers. A sensitivity study has been carried out for the V1 model to obtain the minimum diameter of the hangers from which it can be considered that the ratio between the arch and the deck deflections is close enough to one. When this situation occurs (the so-called "curtain effect"), the loads are effectively transferred from the deck to the arch without increasing the deck forces and deflections too much. Details of a similar study can be found in [13].

With the objective of illustrating the studied structural behavior, the following load cases have been considered in this study:

- The self-weight (*SW*) of the bridge, evaluated for a specific weight of 78.5 kN/m^3, and a dead load (*DL*), with a value of 3.75 kN/m^2.
- Three downward pedestrian live loads distributions, q_1, q_2, and q_3, which correspond to the LM-4 load model defined in Eurocode 1-2 [17] (Figure 6a).
- The wind load (*W*) (Figure 6b) has been considered in a simplified way, as an equivalent static transversal loading (parallel to the Y-axis) of 2 kN/m, acting both at the centroids of the cross-sections of the arch and the deck.

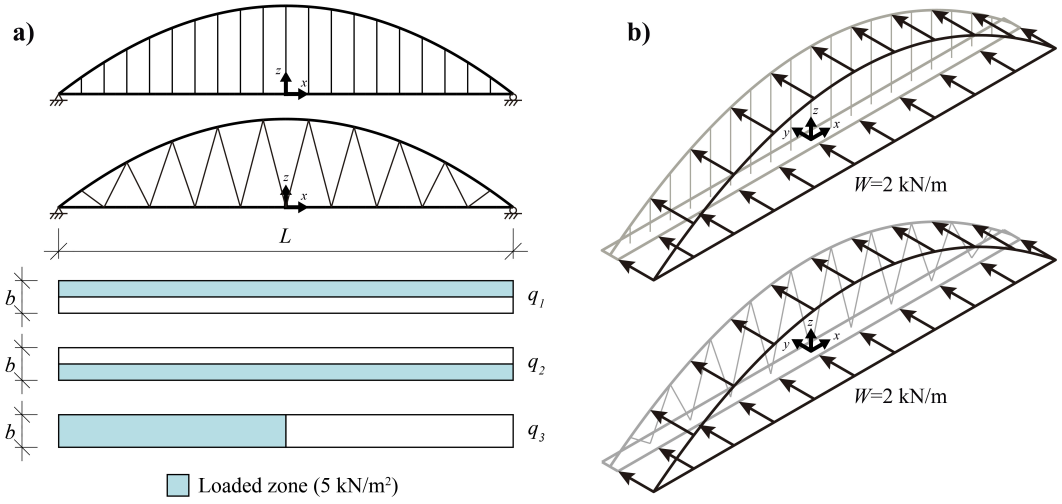

Figure 6. Live loads considered: (**a**) pedestrian live loads; (**b**) wind load.

The load cases defined are illustrative enough of the response of the studied bridges. The response of these bridges under other types of loads will be qualitatively similar. For example, the loads q_1 to q_3 defined in the paper will produce very similar effects to the uniformly distributed loads (UDL system) of Load Model 1 from Eurocode 1-2 [17], although the double-axle concentrated loads (tandem system (TS)) of the same Load Model will have a much more concentrated response. Similarly, the wind load defined in the paper will produce a response similar to that of a transversal seismic action simplified as a pseudostatic load case.

The response of the models has been determined by applying the finite-element method. For this purpose, linear elastic analyses have been carried out under static loads. The models are three-dimensional, with six degrees of freedom per node and are composed of linear members ("frame elements" in SAP2000 [18]).

3. Structural Behavior of the Tied-Arch Bridge with One Set of Central Hangers

This section shows the behavior of bridges V1 and N1. The results of this section are compared with the results of the studies carried out in Section 3, Section 4, Section 5, Section 6, Section 7. This section also exemplifies the problems, mentioned above, that can appear in them. Regarding longitudinal bending (Figure 7), the behavior of bridges such as the V1 is well known, and the most adverse load case corresponds to q_3 (Figure 6). In the V1 bridge, the bending moment diagram both at the arch and the deck has the well-known S-shape. Global bending is shared by the arch and the deck. The proportion of the global bending moment supported by the arch is proportional to $EI_A/(EI_A + EI_D)$, where EI_A and EI_D correspond to the flexural stiffness of the arch and the deck, respectively. The same applies to the deck (see Menn [19]). Regarding the N1, the reduction of bending achieved with respect to the V1, thanks to the Nielsen-type cable arrangement, is very high, around 70% for the bridge studied, both for the arch and deck.

Regarding deflections, and consistently with the results of bending, in Figure 8, it is shown how, under q_3, the N1 model has a much smaller deflection at the centerline of the deck than that of the V1 model. At a point located at a quarter of the span ($x = -L/4$), the vertical deflection reduction is 72%. Logically, the deflections at the edge, δ_E, for the load q_3 are identical to the deflections at the axis of the deck, δ_D, since the distribution of the live load q_3 is symmetric with respect to the plane of the arch.

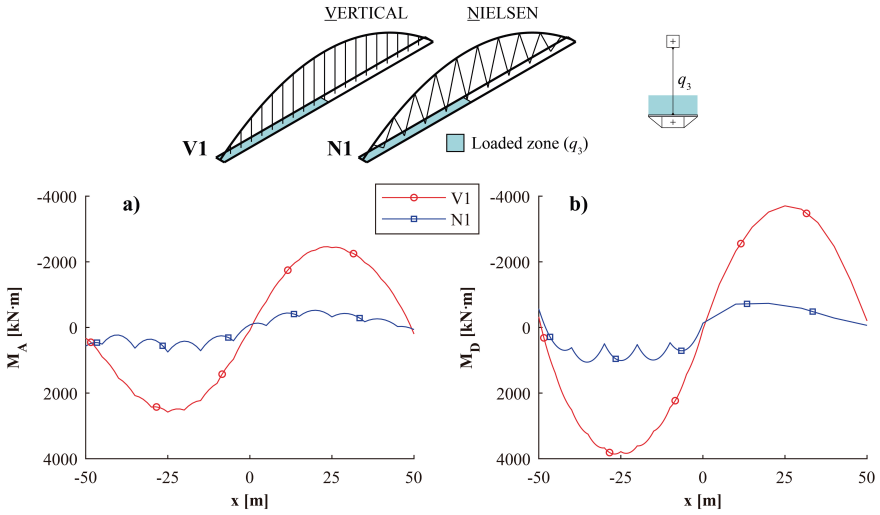

Figure 7. Longitudinal bending under q_3 at the arch (**a**) and the deck (**b**) for V1 and N1.

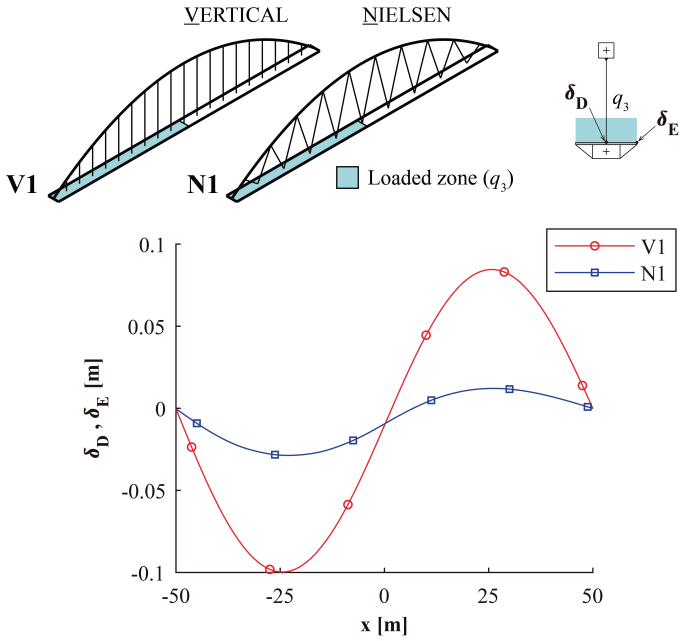

Figure 8. Deflections under q_3 at the deck for V1 and N1.

However, for the q_2 load (Figure 9), at the center of the span ($x = 0$ in Figure 9a), the deflection at the edge of the deck, δ_E, is approximately 2.5 times that of the deck axis, δ_D. This is because the eccentric live load q_2 can be resolved into a downward vertical load and a torsional moment, as shown in Figure 10. Subsequently, the deflection at the edge of the deck, δ_E, can be resolved into two addends:

$$\delta_E = \delta_D + \theta \cdot \frac{b}{2} \tag{1}$$

where δ_D is the deflection on the deck axis and θ is the torsional twist of the cross-section (Figure 10b). δ_D depends only on the global stiffness of the arch-deck vertical structural system, whereas θ depends only on the torsional stiffness of the deck. That means that θ is independent of the hanger arrangement when it is attached to the axis of the deck.

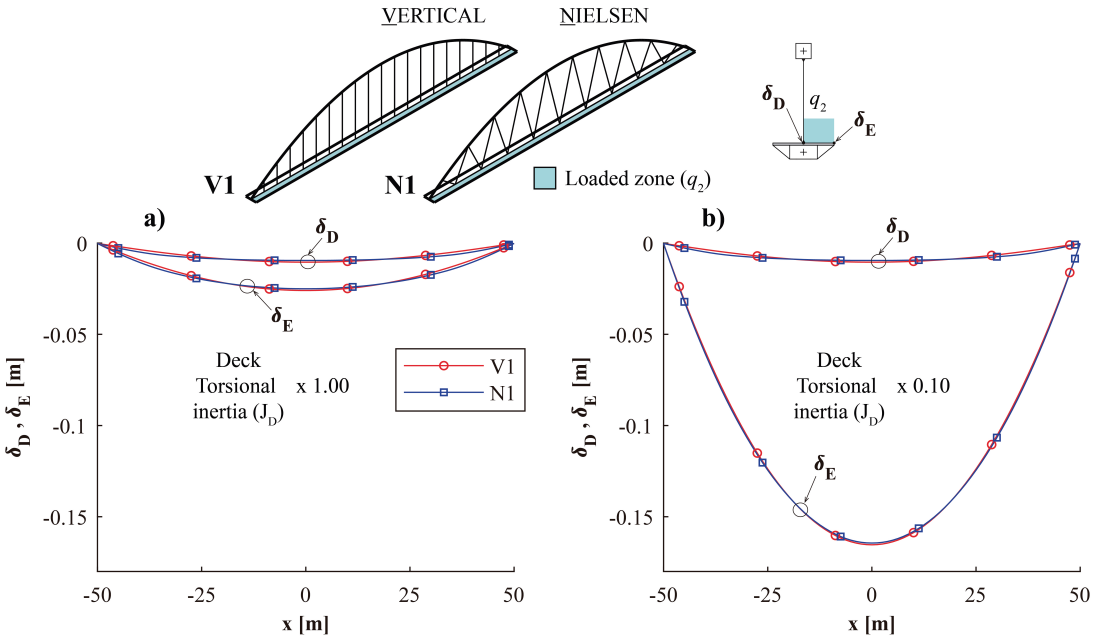

Figure 9. Models V1 and N1: deflections at the axis and edge of the deck for load q_2. Deck torsional stiffness factored by (**a**) 1.00 and (**b**) 0.1.

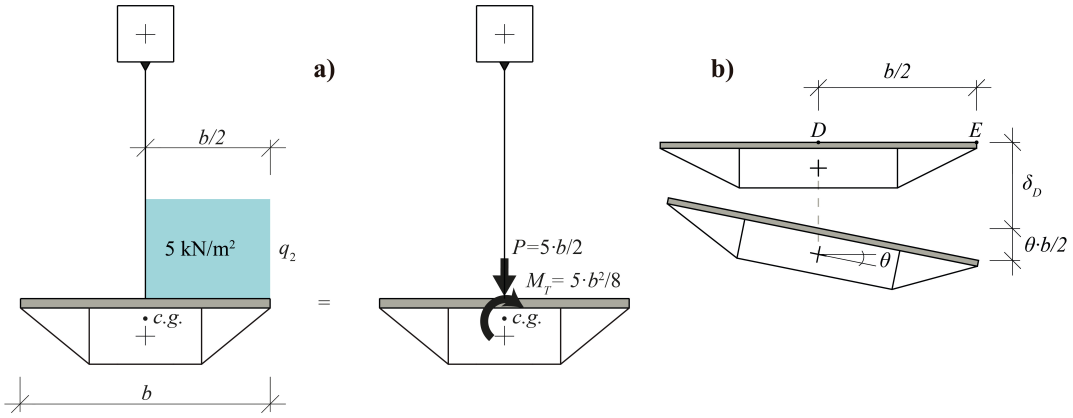

Figure 10. (**a**) Set of forces equivalent to q_2 for models V1 and N1. (**b**) Deflection of the deck and torsional twist of the cross-section.

Therefore, it may happen, if the deck is not torsionally stiff enough, that the most adverse scenario to satisfy the serviceability criteria is not the deflection at quarter spans ($x = \pm L/4$) under q_3 but the deflection at midspan ($x = 0$) under q_2. In other words, even in a bridge with high vertical rigidity, such as the N1, with the Nielsen-type arrangement, a problem could appear at the edge of the deck due to excessive deflections. To illustrate this, Figure 9b shows how the deflection at the deck edge, δ_E, is extremely increased when the torsional stiffness of the deck cross-section is reduced to 10% of its original value, and, subsequently, the difference $\delta_E - \delta_D$ is 10 times higher than that shown in Figure 9a.

Several design strategies can be used to tackle these design problems. As it was previously mentioned in the Introduction section (Section 1), the main design strategies are: increasing the size of the deck cross-section; duplicating the arches and placing them at the edges of the cross-section; stiffening transversally the hangers, and, finally, doubling the set of hangers and attaching the arch to both edges of the deck, which is the focus of the research shown in this paper, and introduced in the next section.

4. Structural Behavior of the Tied-Arch Bridge with Two Sets of Lateral Hangers

In this section, two bridges, V2 and N2 (Figure 11), are analyzed, which differ from V1 and N1 respectively, in that they have two sets of hangers, each one attached to an edge of the deck. Obviously, the geometry of the cable arrangement must not interfere with the deck clearance in order to allow both pedestrian and vehicular traffic. Sometimes, this restriction may lead to the introduction of additional width in the deck. In this research, it has been assumed that the geometries shown in Figure 11 meet this requirement. The dimensions of the cross-sections and the hangers are the same as already defined in Table 1.

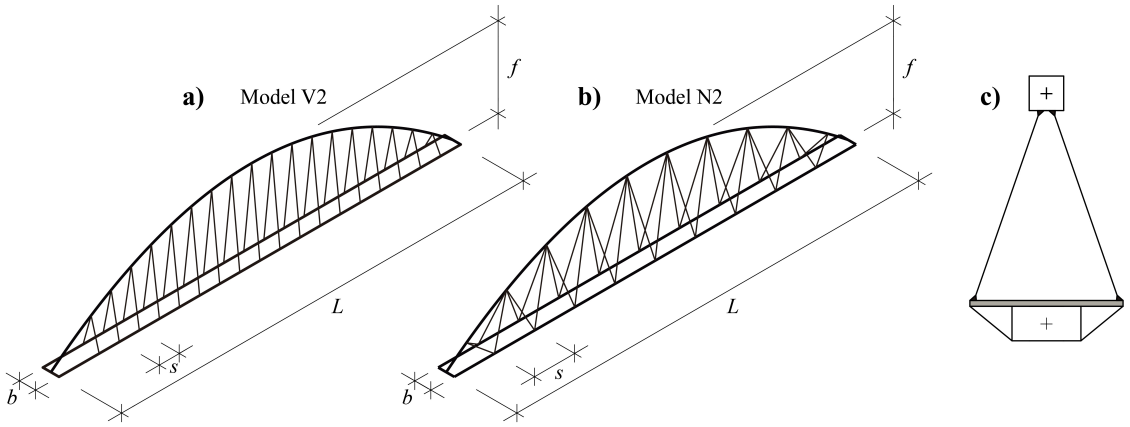

Figure 11. (**a**) Model V2; (**b**) model N2; (**c**) cross-section.

Figure 12 compares the deflections for bridges V2 and N2 with those of bridges V1 and N1, already shown in Figure 8. For the asymmetric longitudinal load q_3 (Figure 12), the deflections are virtually identical for models V1 and V2 and very similar for models N1 and N2. The difference can be attributed to the slight increase in the vertical rigidity of N2 with respect to N1 provided by the additional set of hangers. It should be noted that the Nielsen-type cable arrangement keeps the efficiency that has already been shown for the N1 when reducing deflections.

However, regarding the deflections at the edge of the deck due to a live load on the half of the deck distributed over the entire span, such as q_2, it is shown in Figure 13a that the deflections for bridges V2 and N2 are much smaller (about 50% for the bridges studied) than for the bridges N1 and V1 with central hangers, previously shown in Figure 9a. In fact, even if the torsional inertia of the deck is reduced to a mere 10% of its original value (Figure 13b), the deflections at the edge of the deck of bridges N2 and V2 are only moderately higher than those obtained for the original stiffness. This happens because, in the bridges with two sets of hangers, the torsion due to the eccentricity of q_2 is not only supported by the deck, as it is the case in bridges V1 and N1, but also by the axial forces of the hangers attached to the edges of the V2 and N2 decks. The structural systems involved in this structural behavior are detailed in Section 5. Figure 14b shows how the torsion in the deck is lower in bridges N2 and V2 than in bridges V1 and N1. This is consistent with the mentioned fact that, in bridges N2 and V2, the deck resists only a fraction of the torsion under q_2.

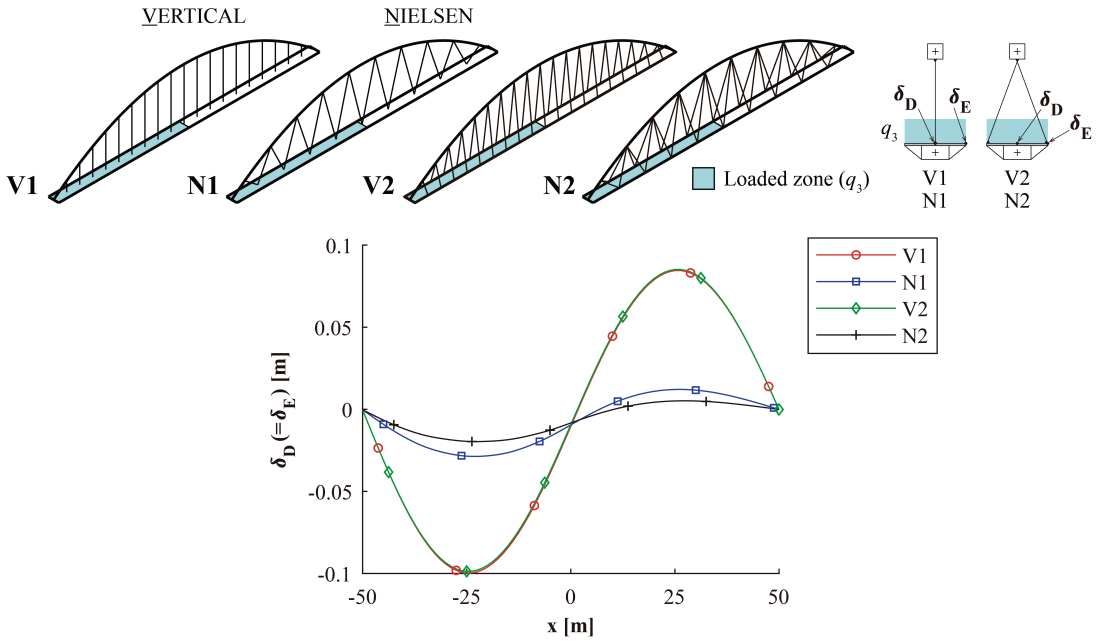

Figure 12. Deflections at the deck axis (and edges) for q_3.

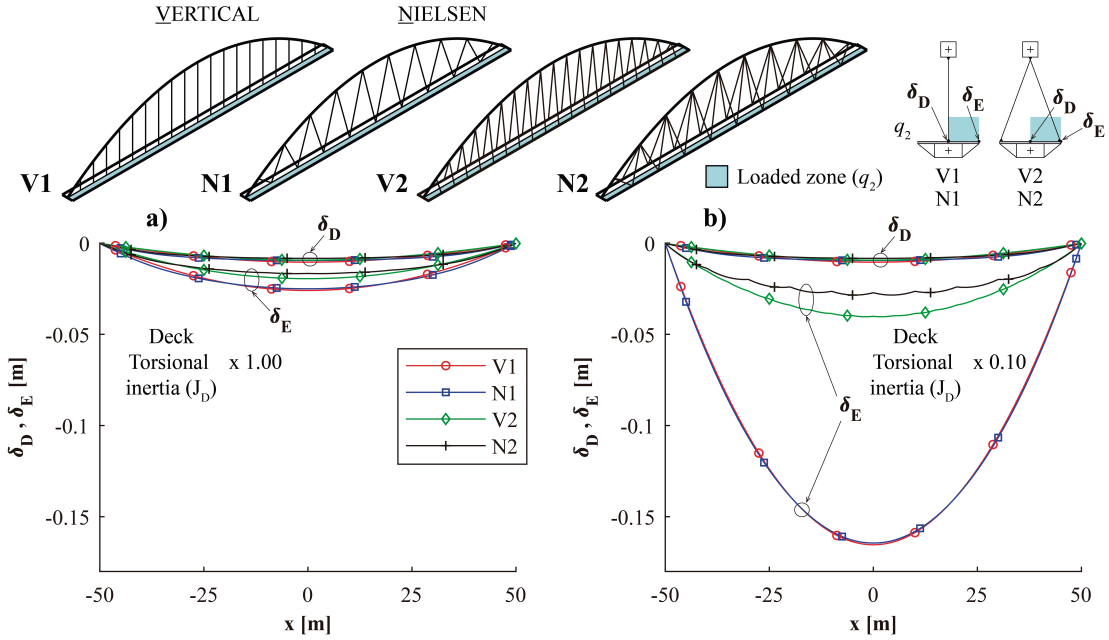

Figure 13. Deflections at the axis and edge of the deck for q_2. Deck torsional stiffness factored by (**a**) 1.0 and (**b**) 0.1.

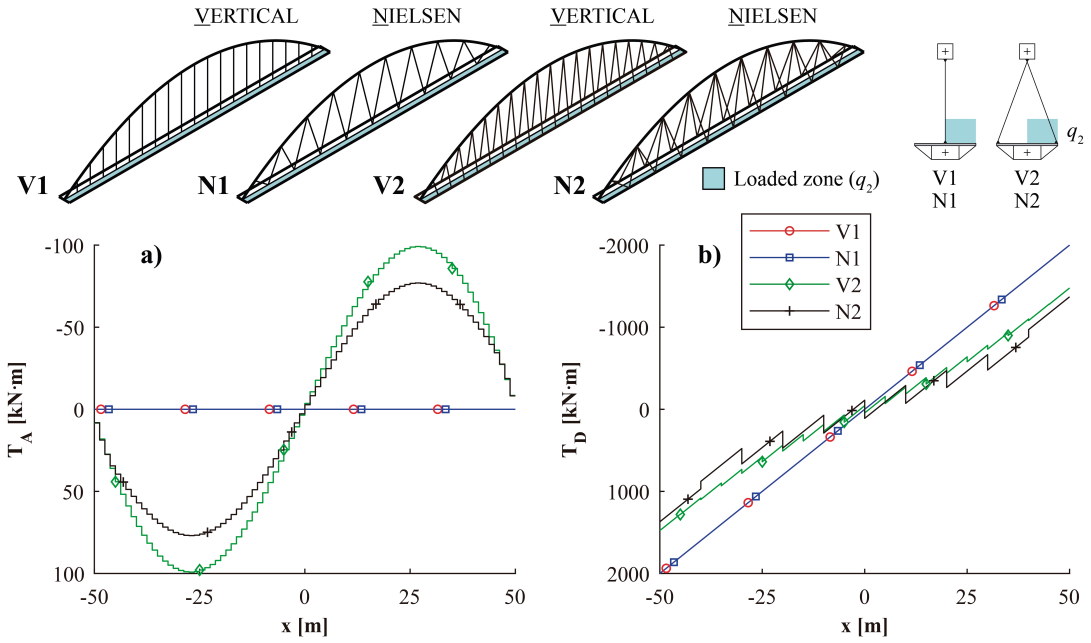

Figure 14. Torsion at the arch (**a**) and the deck (**b**) for q_2.

Since, under q_2, the axial forces of the hangers attached to the same location of the arch are different, in bridges with two sets of hangers, the torsion in the deck causes out-of-plane bending in the arch (Figure 15a) and vertical-axis bending moments at the deck (Figure 15b). Note that this bending does not appear in bridges N1 and V1 neither at the arch nor at the deck (Figure 15). Similarly, in bridges V1 and N1, where the hangers are attached to the center of the deck, there is no reduction in torsion (Figure 14b). Torsion appears in the arch for q_2 (Figure 14a) by coupling with the out-of-plane bending, as in any curved member. It appears when it is loaded by the out-of-its-plane components of the hangers.

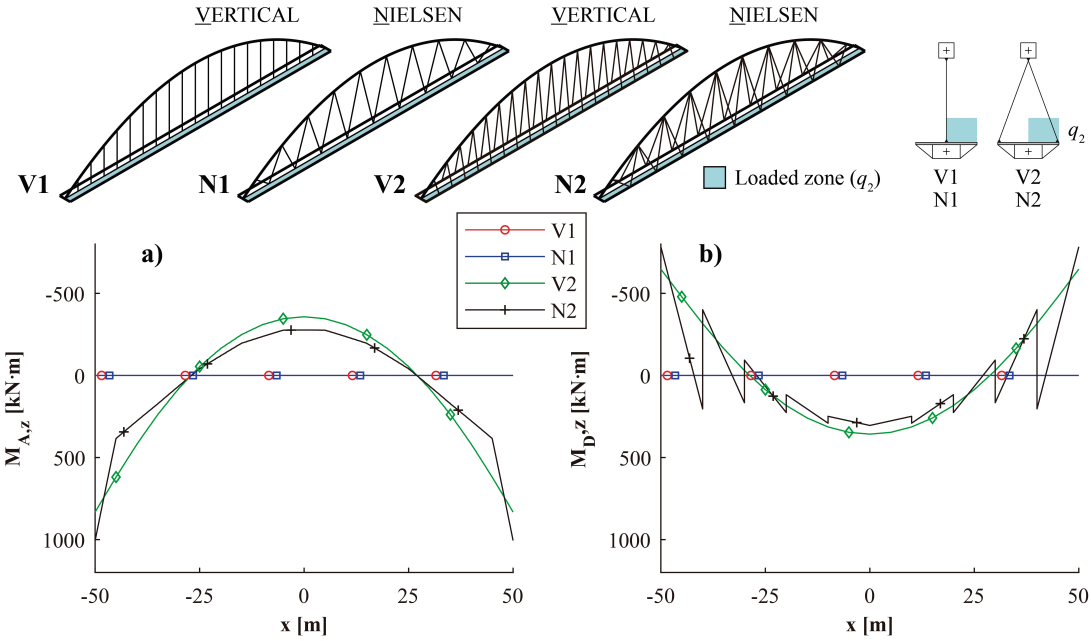

Figure 15. Bending under q_2. (**a**) Out-of-plane bending at the arch. (**b**) Vertical-axis bending at the deck.

The transversal behavior of both the arch and the deck becomes evident when their transversal displacements are analyzed (Figure 16). In both N2 and V2 bridges, the arch gets closer to the loaded

area while the deck separates from it. It should be noted that for V1 and N1 there is no transversal displacement neither of the arch nor of the deck.

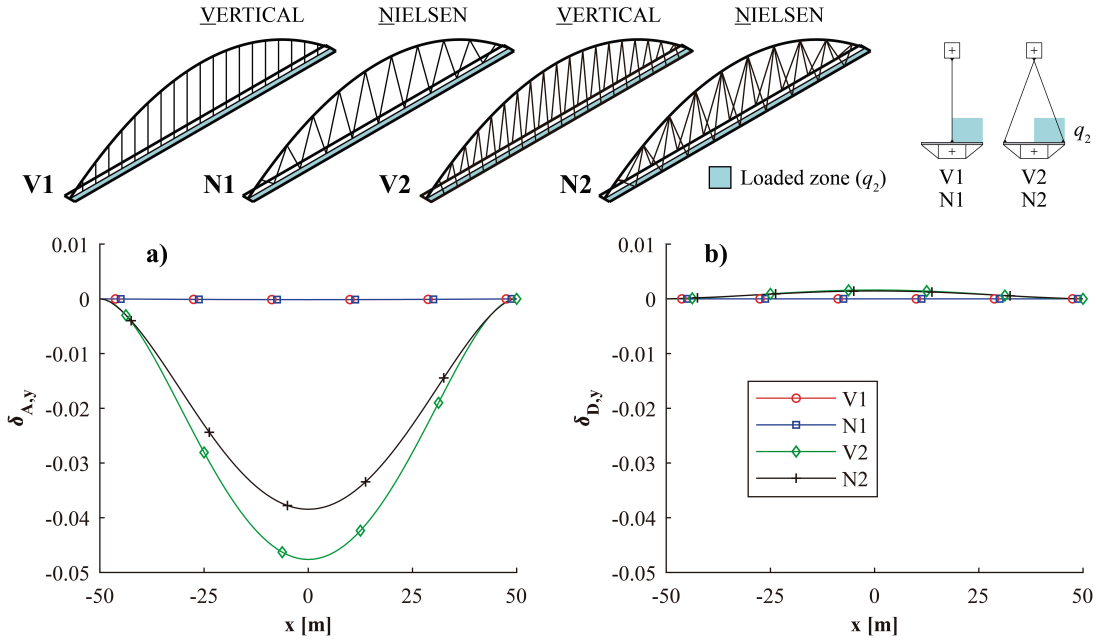

Figure 16. Lateral displacements under q_2 (**a**) at the arch and (**b**) the deck.

As expected, the longitudinal bending for q_3 is consistent with the behavior of the deflections and remains almost unchanged (Figure 17) between the models V1 and V2 and the models N1 and N2, except for the influence of the second set of hangers.

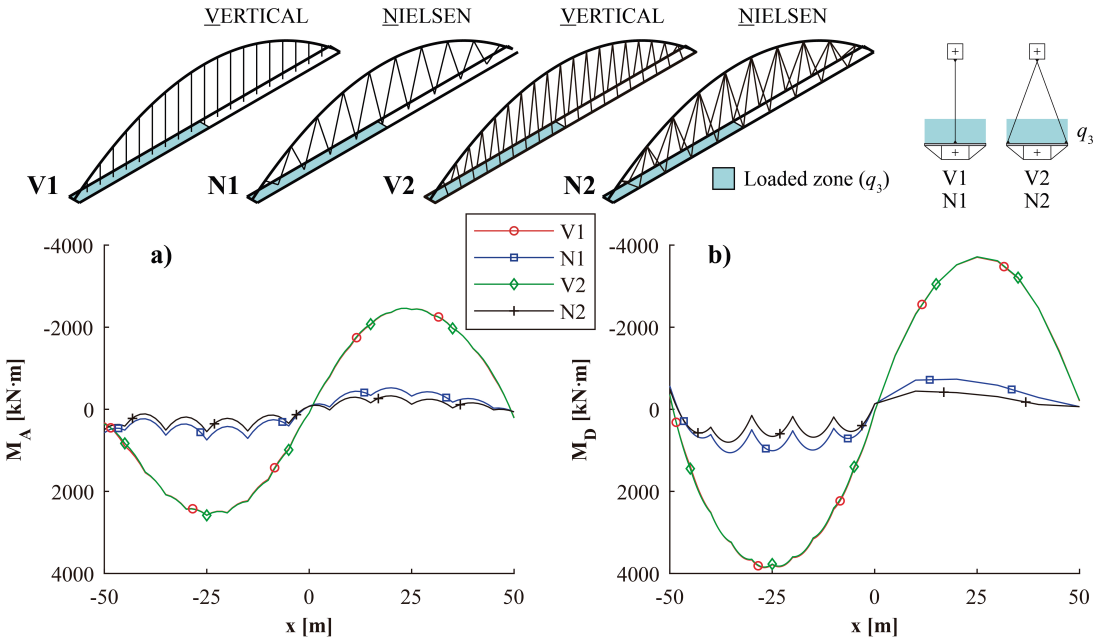

Figure 17. Longitudinal bending under q_3 at the arch (**a**) and the deck (**b**) for V1, N1, V2, and N2.

The wind load causes out-of-plane bending in the arch (Figure 18a), vertical-axis bending in the deck (Figure 18b), as well as torsion in the arch and the deck (Figure 19). In bridges V1 and N1, the hangers do not contribute to resisting the wind action since they are perpendicular to the wind direction. However, in bridges V2 and N2, the inclined hangers make both the arch and the deck

resist jointly. This reduces the transversal bending in both the arch and at the deck ends in N2 and V2 (Figure 18) as compared to that in N1 and V1. In Figure 20, the transversal displacements of the arch and the deck due to the wind are shown, and it can be noted that, in the arch, they are much smaller for V2 and N2 than for V1 and N1.

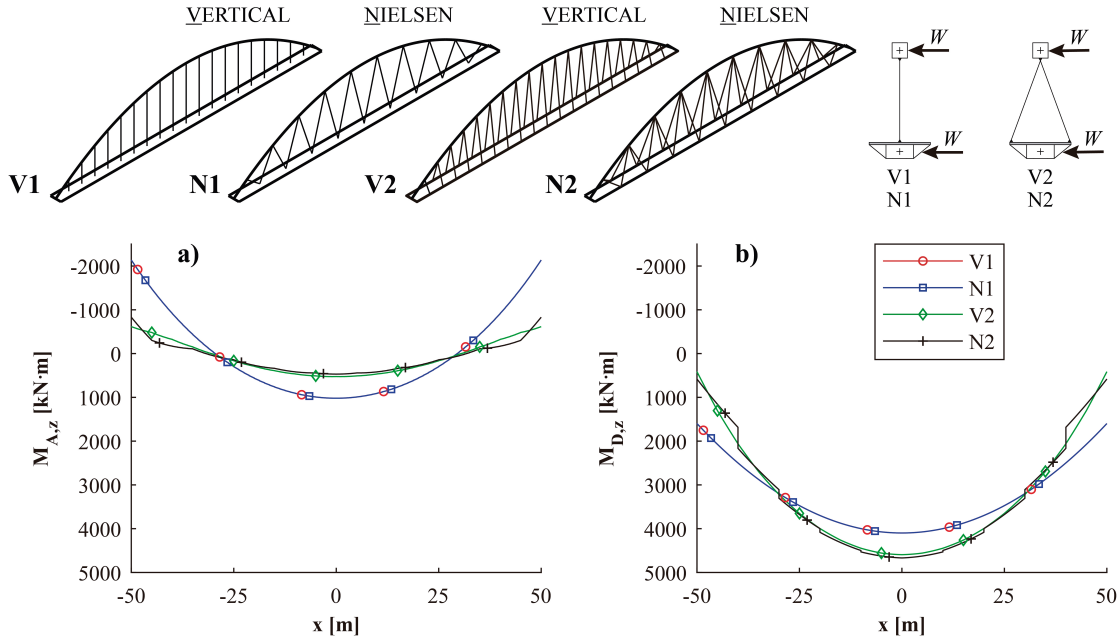

Figure 18. Transversal bending under wind loading. (**a**) Arch, (**b**) Deck.

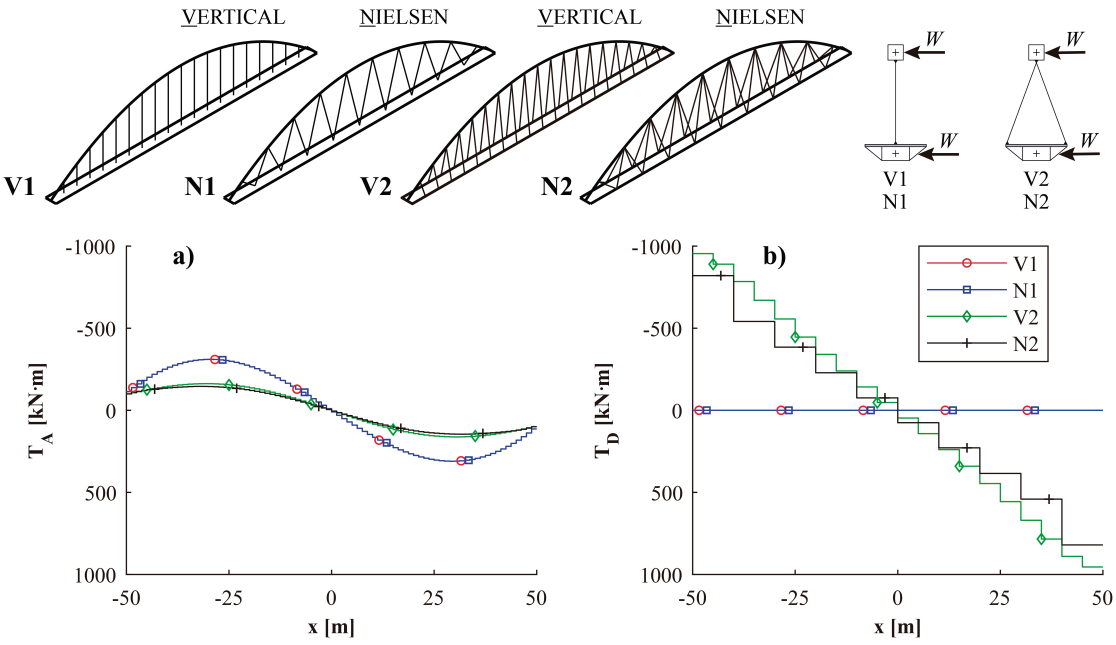

Figure 19. Torsion under wind loading: (**a**) arch; (**b**) deck.

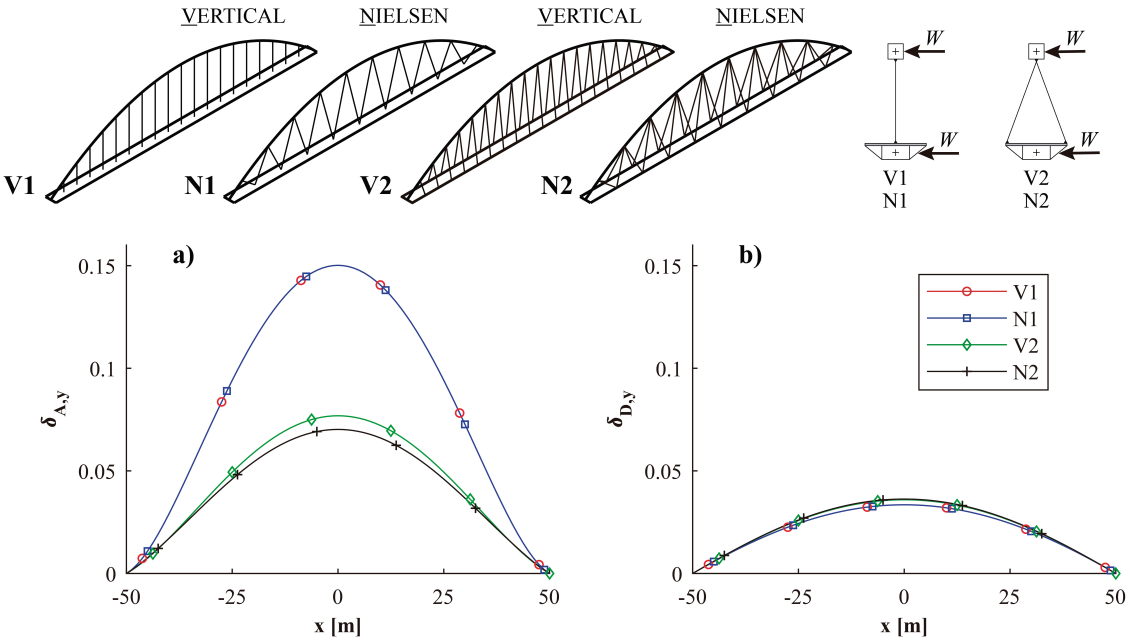

Figure 20. Transversal displacements under wind loading: (**a**) arch; (**b**) deck.

5. Structural Systems in the Studied Bridges

In light of the results of the previous sections, the structural systems that carry the loads for the bridges studied in this paper are analyzed below. Since the cross-sections of both the arch and the deck are doubly symmetrical, the structural behavior of the studied bridges can be resolved into two: a structural behavior within the vertical plane containing the arch and an out-of-plane behavior (Jorquera-Lucerga [20]). To help understand the structural behavior of these bridges, and from an exclusively intuitive approach, Figure 21 shows the projections of the V2 and N2 bridges. The vertical projection of the V2 bridge is a V1-type bridge and, in the horizontal plane, resembles a Vierendeel beam. Similarly, the vertical projection of the N2 is an N1-type bridge and, in plan, it forms a three-chord truss connected by diagonals that are the projection of the hangers on a horizontal plane.

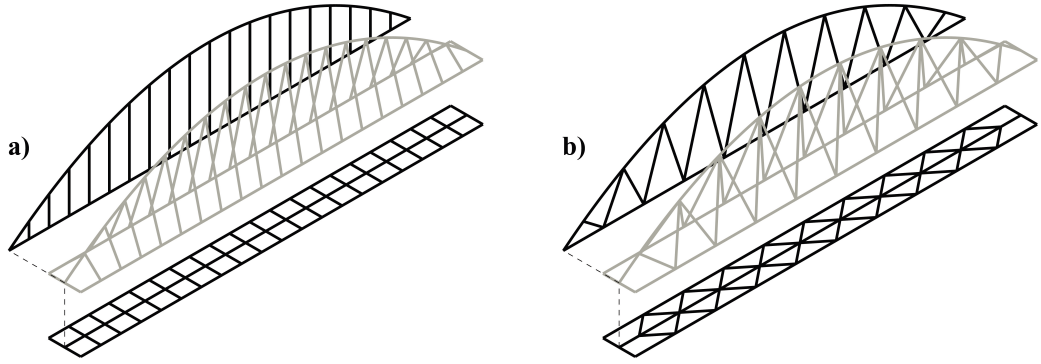

Figure 21. Vertical and horizontal projections of (**a**) V2 and (**b**) N2 bridges.

The structural systems of the bridge with two sets of cables become particularly evident when, under any nonsymmetrical load with respect to the plane of the arch, the axial loads of the hangers attached to the same location of the arch are different. For example, in a V2 bridge, two hangers coincide at the same point of the arch, whose axial loads are P_a and P_b. Figure 22 illustrates the forces transferred by these hangers to the arch and the deck when $P_a > P_b$. It illustrates how the study can then be split up by analyzing separately the vertical behavior (under loads whose resultant are

contained within the plane of the arch, such as q_3) and the transversal, or out-of-plane, behavior (under eccentric loads, such as q_1 or q_2, or out-of-plane loads, such as the wind load).

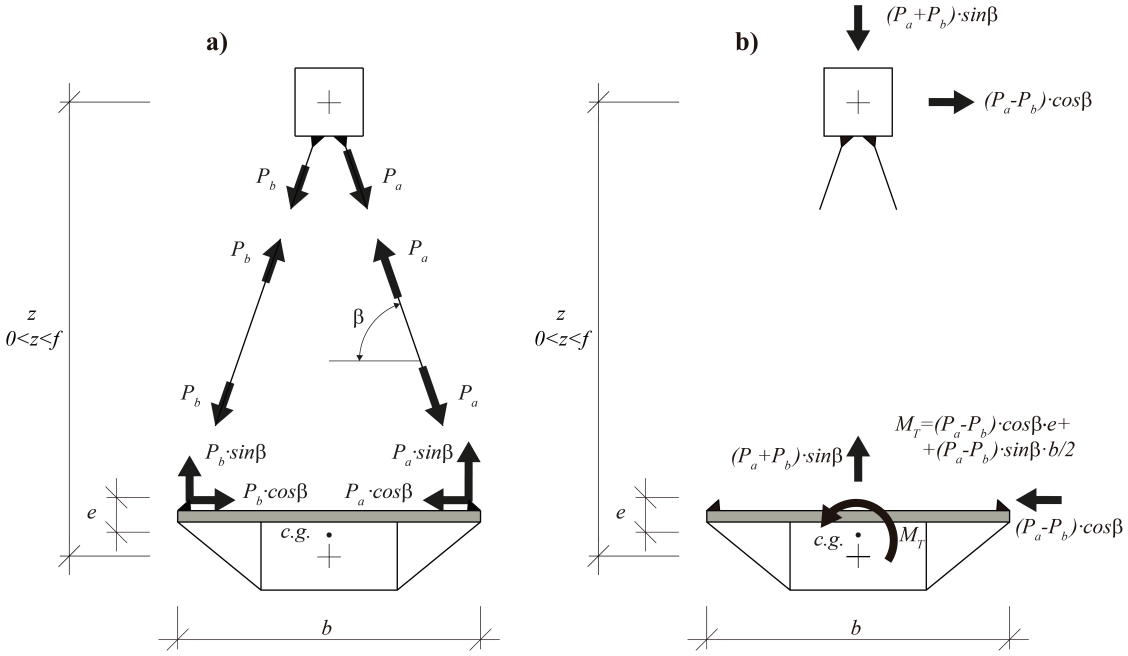

Figure 22. Transversal effect of axial forces at hangers for the V2 bridge when $P_a > P_b$. (**a**) Forces transferred by the hangers. (**b**) Resultant forces.

5.1. Actions Contained within the Plane of the Arch

The in-plane behavior of bridges with two sets of cables is very similar, as has been shown, to that of bridges with one central set of cables, except for the fact that it must be considered that the hanger arrangement has been doubled. It can be stated that when the bridge with a doubled hanger set (i.e., a V2 or N2-type) is loaded exclusively with actions contained within the plane of the arch, it behaves as an arch with a simple set of hangers (i.e., a V1 or N1-type) where the equivalent $\Omega_{H,\alpha}$ area of each hanger (Figure 23a) is obtained according to the following expression, adapted from Ortiz-Berrocal [21]:

$$\Omega_{H,\alpha} = 2 \cdot \Omega_H \cdot cos^3(\alpha) \quad (2)$$

where α is the angle between the hanger and the plane of the arch (Figure 23b).

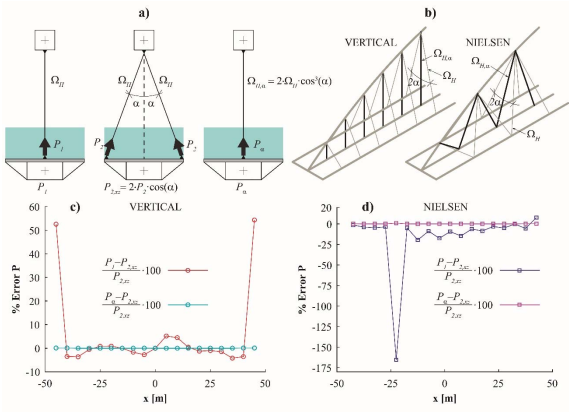

Figure 23. (**a**) Equivalent area of hangers and compared axial loads. (**b**) Definition of α. (**c**) Comparison of results for vertical arrangement and (**d**) Nielsen arrangement.

To verify the validity of this assumption, Figure 23c compares, under the load q_3, the axial load P_α to the axial load $P_{2,XZ}$ (Figure 23a). P_α corresponds to the axial load at a given hanger of an equivalent bridge with one central cable arrangement, obtained by transforming a V2-type bridge into a V1-type bridge where the areas of the hangers are obtained according to Equation (2). $P_{2,XZ}$ is the projection on the plane of the arch (that is, on the vertical plane) of the axial forces of the two hangers that form an angle of α with the plane of the arch and are anchored at the same point of it. Similarly, $P_{2,XZ}$ is compared to P_1, which is the axial load at a given hanger of the V1-type bridge.

Firstly, as previously studied, Figure 23c shows how, for q_3, $P_{2,XZ}$ and P_1 are slightly different (less than ±10%), except near the ends of the bridge, where the variations are greater than 50%. However, the axial loads $P_{2,XZ}$ are very similar to the axial loads P_α, with errors, for the bridges studied, below 1%. A similar study has been carried out for the N2 bridge, which also provides very similar results (Figure 23d). The differences between $P_{2,XZ}$ and P_1 are under 25%, except in only one hanger, and the differences between $P_{2,XZ}$ and P_α are also below 1%. The results both for N2 and V2 bridges confirms the validity of the assumption.

5.2. Out-of-Plane Actions

The out-of-plane actions, whose resultants are shown in Figure 22b, are resisted by the structural systems described in Figure 24. The specific distribution among the different structural systems depends, obviously, on the transversal and torsional rigidities of the arch and the deck. Since the deck width is usually quite larger than that of the arch due to functional reasons, the transversal stiffness of the deck is usually much higher than that of the arch. Therefore, the stiffness of the arch governs the relationship between the axial forces of the hangers. To illustrate this, Figure 25 shows the axial loads of the hangers of the loaded and nonloaded zones, P_a and P_b, respectively, as a function of the transversal stiffness of the arch for eccentric load on the edge of the deck.

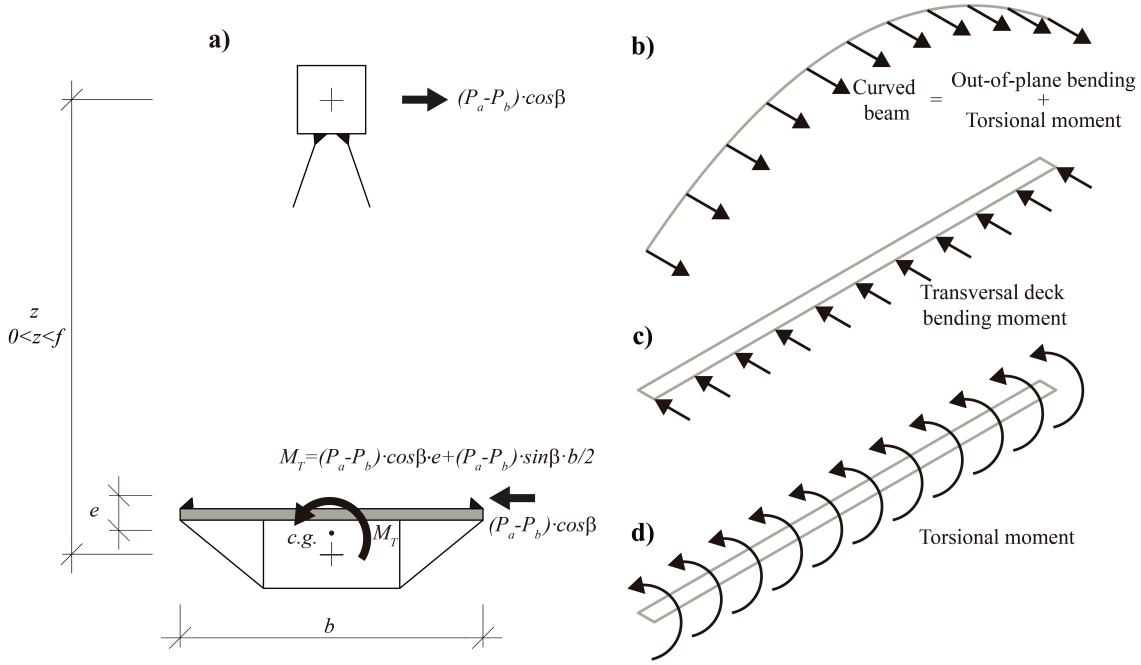

Figure 24. Structural systems for out-of-plane actions in bridges with two sets of lateral hangers. (**a**) Resultant of loads; (**b**) Arch as a curved beam; (**c**) Transversal bending and (**d**) torsion at the deck.

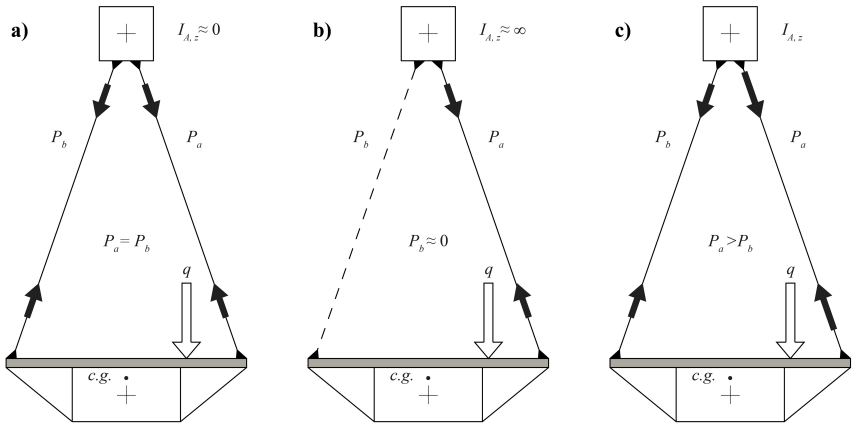

Figure 25. Axial forces at the hangers of a V2 bridge for a load on the edge of the deck as a function of the transversal stiffness of the arch: (**a**) $I_{A,z} \approx 0$; (**b**) $I_{A,z} \approx \infty$; (**c**) actual $I_{A,z}$.

6. The Forked Arch

As described in Sections 4 and 5, in V2 and N2 bridges, under the q_2 load, the axial forces at the hangers attached at the same location of the arch are different. As has been shown, the orientation of the horizontal components of the axial forces makes the arch move towards the loaded side whereas the deck separates from it. As discussed in Section 5, the deck behaves as a beam with the same span as that of the arch subjected to vertical-axis bending, whereas the arch acts as a curved member in which torsion appears by coupling. However, the arch and the deck are rigidly connected at their ends, and, therefore, bending moments are developed at those intersections because the deck and the arch prevent each other from rotating. In the V2 bridge, the hangers are contained in vertical planes parallel to the *Y*-axis. That is, the hangers are not able to support part of the moment appearing in the arch-deck intersection, which is fully supported by the arch and by the deck. However, in the N2 bridge, the hangers, which are contained within diagonal planes with respect to the X-axis, do have some capacity to develop a force couple and support part of the moment. Therefore, it may happen that, in the N2 bridge, the hangers closest to the ends of the arch go into compression.

To confirm this, Figure 26 shows, for the V2 and N2 bridges and for the q_2 load, the axial forces P of the hangers, where P_a corresponds to the hangers closer to the loaded side and P_b to the nonloaded side of the deck. As can be seen, the axial forces P_a are, in general terms, higher. However, the most important aspect is that in the N2 bridge, the axial forces of two hangers near the ends go in compression, which indicates that, at each end of the bridge, the vertical-axis moment is partially resisted by the force couple generated by the hangers.

This can be avoided by forking the arch (Figure 27) so that the bending moment shown in Figure 26 can be supported by a force couple, composed of a compressive and a tensile force, each one acting at each leg of the arch. An example of this Nielsen-type solution is the Montigny-Les-Cormeilles footbridge (Figure 28), designed by Michel Virlogeux. In this footbridge, in addition, the deck section is made up of two longitudinal beams placed at the edges of the deck, tying the springing points of each leg of the arch (see Oudin-Hograindleur et al. [22]).

Although the problem of the hangers entering into compression is something inherent to N2-type bridges, there are also bridges with vertical cable arrangements where the arch has been forked, such as the Wittenberg Bridge, shown in Figure 4. In the Third Millennium Bridge (Figure 29b), in Saragossa (Spain), the forked tied-arch is made up of concrete and is attached to both edges of the deck (Sacristán et al. [23]), whereas in the Barqueta Bridge (Figure 29a), the arch is made up of steel and attached to the axis of the deck (Arenas de Pablo and Pantaleón [24]). However, in this case, beyond structural considerations, the intention of the designer, Juan José Arenas, was to create a "gate effect" under the arch for the pedestrians entering the 1992 Seville Exhibition. Secondarily, when the arch is forked, its buckling length is reduced, as will be discussed in the next section.

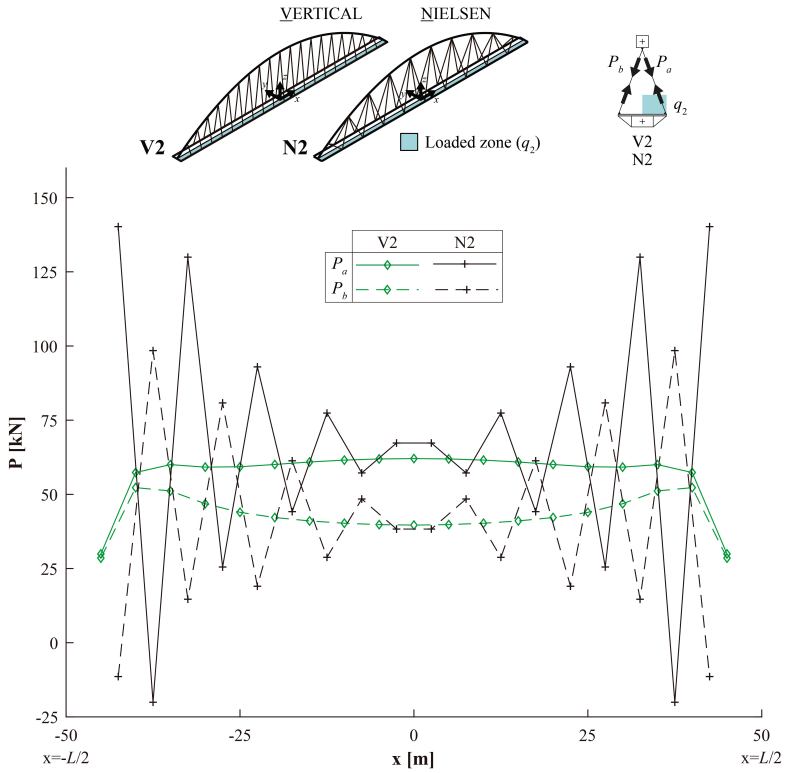

Figure 26. Axial loads at hangers located at both sides for bridges N2 and V2 under q_2 loading.

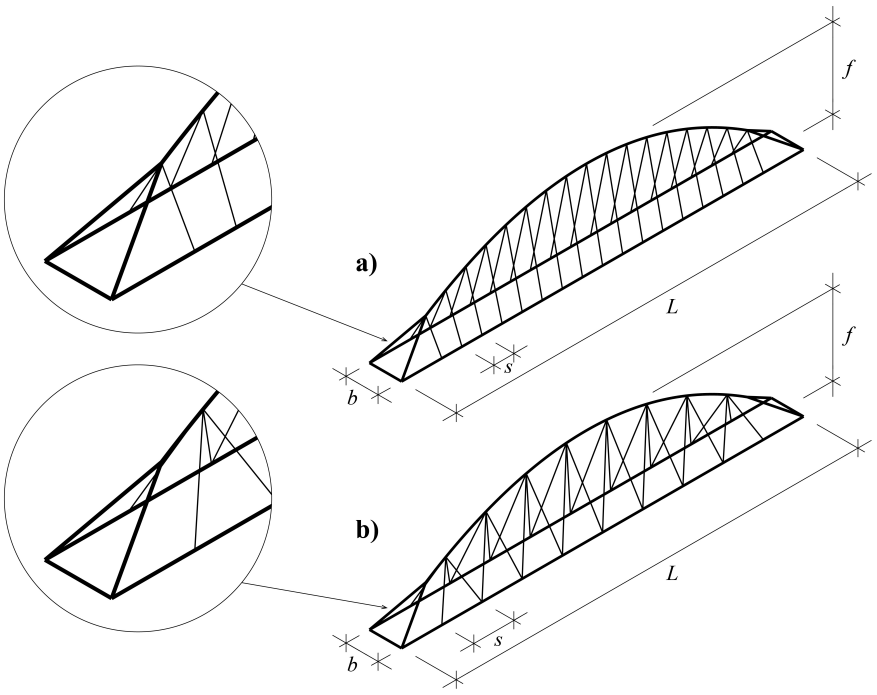

Figure 27. Forked arch for vertical cable arrangement (**a**) and for Nielsen cable arrangement (**b**).

Figure 28. Montigny-Les-Cormeilles footbridge, France. Photo: Google Maps, Street View.

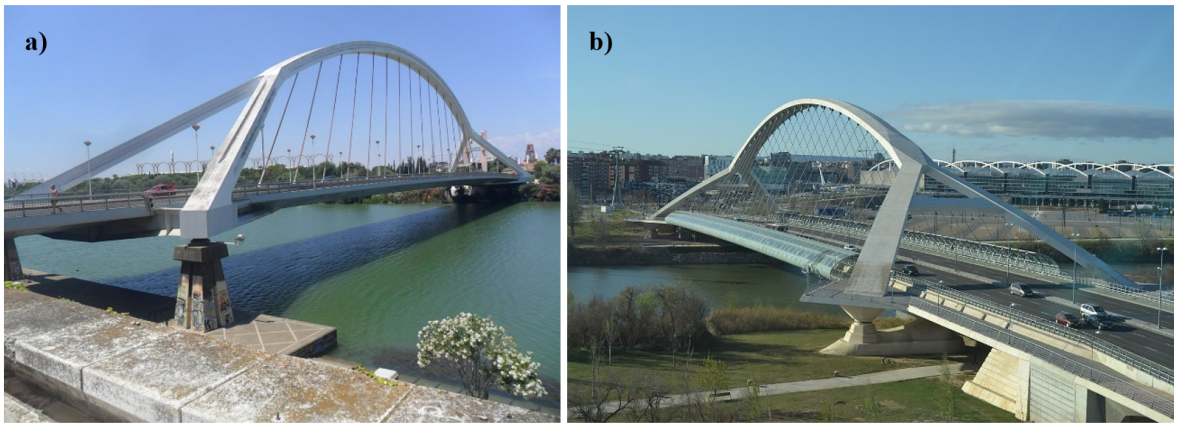

Figure 29. (**a**) La Barqueta Bridge, Seville, Spain. Photo: Juan José Jiménez, Wikimedia Commons. (**b**) Third Millennium Bridge, Saragossa, Spain. Photo: edu1975, Wikimedia Commons.

7. Buckling

This section studies the effect of the hanger arrangement on the critical buckling load. In addition to the bridges V1, V2, N1, and N2, the bridges FV2 and FN2 have also been studied. The bridges FV2 and FN2 are obtained, respectively, by forking the arches and by splitting the central hollow-box cross-section of the deck of the V2 and N2 bridges into two hollow-box rectangular cross-sections of half the width, each one at an edge of the deck, as shown in Figure 30.

In this study, the critical out-of-plane buckling load has been obtained, which is the governing buckling mode. The geometric imperfections have been considered according to the Spanish Structural Steel Instruction EAE [25], which coincides with the values defined in Annex D to EC 3-2 [16]. All models have been analyzed with a linear buckling analysis in SAP2000 [18], which considers geometrical nonlinearity and postprocessed in MATLAB [26] under the Q_b loads combination:

$$Q_b = 1.35 \cdot (SW + DL) + 0{,}6 \cdot 1.5 \cdot W + \lambda_u \cdot (q_1 + q_2) \quad (3)$$

where λ_u is the load factor that multiplies the live load $q_1 + q_2$ (i.e., the whole deck loaded) at the moment of buckling (Manterola-Armisén [8]). The values of λ_u for all cases are shown in Table 2.

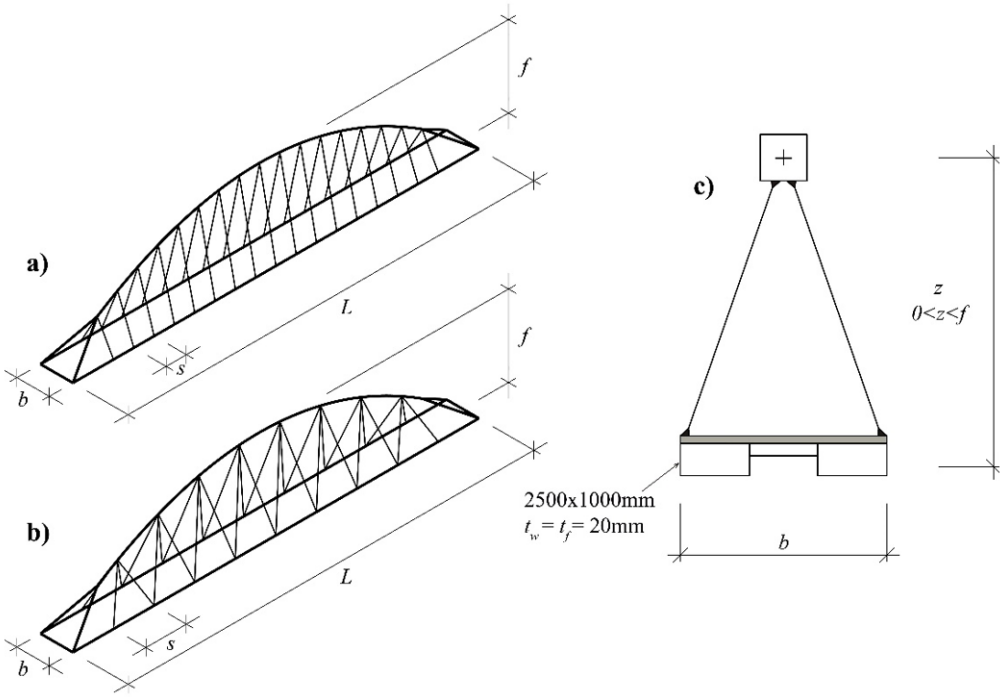

Figure 30. Definition of (**a**) FV2 and (**b**) FN2 bridges. (**c**) Cross-section for FV2 and FN2 bridges.

Table 2. Minimum factors of $q_1 + q_2$ to achieve out-of-plane buckling.

Model	λ_u
V1	11.2
N1	11.2
V2	24.1
N2	28.0
FV2	37.5
FN2	42.0

As can be seen in Table 2 and Figure 31, the models with a central set of hangers (V1 and N1) present the lowest values of λ_u, with hardly any difference between them. In the case of the models with two sets of lateral cables (V2 and N2), λ_u increases notably, becoming, in the bridges studied, at least twice as much as in the case of V1 and N1. This increment appears because the cables, inclined and attached to a deck with high transversal stiffness, tend to prevent the arch from displacing transversally. The highest values of λ_u correspond to the forked arch bridges (FV2 and FN2) because of a double effect: on the one hand, the transversal stiffness of the deck is higher because the cross-section of the deck is split into two separate halves, and, on the other hand, the triangular cells at the ends reduce the buckling length of the arch.

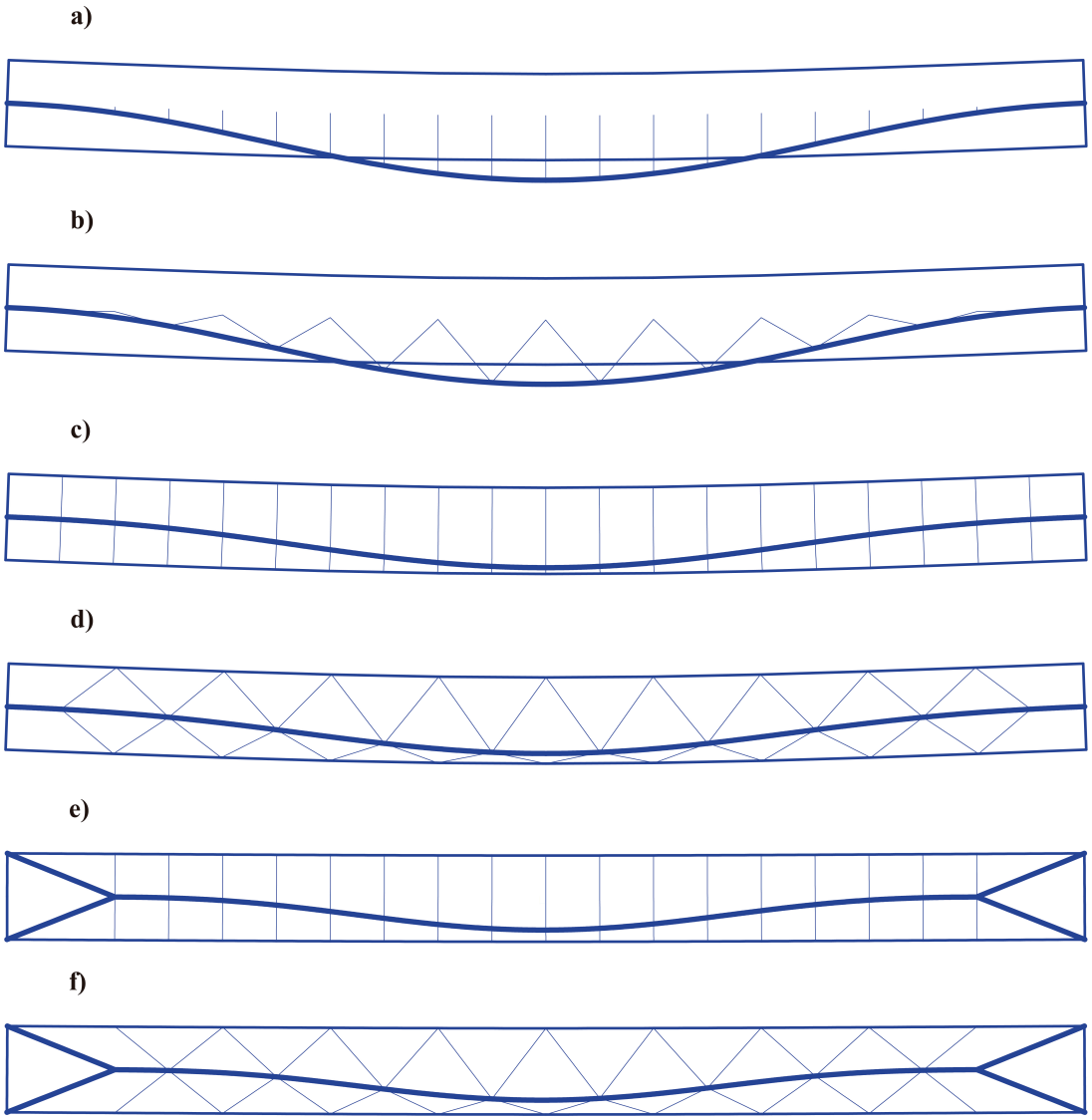

Figure 31. Out-of-plane buckling of the studied papers. (**a**) V1, (**b**) N1, (**c**) V2, (**d**) N2, (**e**) FV2, and (**f**) FN2.

8. Conclusions

The following conclusions can be drawn from the studies carried out in this research:

In tied-arch bridges, the most frequent method of linking the arch and the deck is by means of a single set of hangers that links the arch and the axis of the deck, using either vertical or Nielsen-type hangers. When properly designed, the cable arrangement can significantly reduce the forces and deflections under symmetrical loads with respect to the plane of the arch, improving the structural behavior in the vertical plane. However, it does not help to solve problems due to nonsymmetrical actions with respect to the plane of the arch, such as eccentric load distributions or wind loading. Furthermore, it does not reduce the sensibility of the arch to out-of-plane buckling.

Thus, this paper studies how a cable arrangement composed of two sets of hangers attached to both edges of a deck can be very suitable to solve the mentioned problems. This arrangement does not worsen the structural behavior of the bridge in the vertical plane under symmetric loads with respect to that of bridges with a single centered set of hangers. In fact, in the studied cases, the structural behavior improves. In this paper, it is demonstrated how the in-plane behavior of a bridge with two sets of cables under symmetrical loads can be accurately reproduced by a bridge with one set of cables,

whose area is a function of the area of the hangers and their inclination with respect to the plane of the arch.

In the bridge with one set of hangers, the deformations of the edge of the deck under nonsymmetrical loads depend, besides the vertical stiffness of the arch-hangers-deck structural system, exclusively on the torsional stiffness of the deck. In this paper, the structural systems that resist nonsymmetrical loads or wind have been identified and described qualitatively. Thus, it is shown how, in bridges with hangers attached to the edges of the deck, the torsion of the deck is also resisted by the transversal stiffness of the deck, as well as by the transverse stiffness of the arch (that is, by its stiffness as a curved beam, governed by its out-of-plane stiffness and its torsional stiffness). This fact decreases the vertical deflections at the edge of the deck. These structural systems cause the arch and the deck to deform transversely under an eccentric load: the arch approaches the loaded area and the deck separates from it.

Similarly, linking the arch with two sets of hangers attached to the edges of the deck reduces the internal forces in both the arch and the deck under the wind load, as well as their transversal displacements.

In Nielsen-type arrangements with two lateral sets of hangers, the end hangers may enter compression since the deck and the arch are rigidly connected at their ends and a bending moment appears. This problem can be solved by forking the arch.

With regard to the out-of-plane buckling of the arch, the critical buckling load is significantly increased by using two lateral sets of hangers with respect to that obtained for bridges with one central set of hangers. This behavior improves further if the arch is forked near its ends since the buckling length is reduced.

Nielsen-type configurations show very efficient in-plane behavior. Similarly, regarding the out-of-plane behavior, many design problems are solved by using two sets of hangers. Since network-type bridges have developed very quickly and are used, nowadays, more frequently than Nielsen bridges, a possible widening of the scope of the research of this paper is the use of a network-type with two sets of hangers instead of a Nielsen hanger arrangement.

Author Contributions: Conceptualization, J.M.G.-G. and J.J.J.-L.; investigation, J.M.G.-G. and J.J.J.-L.; writing—original draft preparation, J.J.J.-L.; writing—review and editing, J.M.G.-G. and J.J.J.-L.; supervision, J.J.J.-L.; funding acquisition, J.J.J.-L. All authors have read and agreed to the published version of the manuscript.

Funding: The authors wish to thank the Universidad Politécnica de Cartagena (UPCT, Spain) for the funding provided, through the research project 2017_2420, directed by the second author.

Acknowledgments: The authors wish to thank the Seneca Foundation (Murcia Region, Spain), for the funding of the first author's research scholarship (FPI).

Conflicts of Interest: The authors declare no conflict of interest. The funders had no role in the design of the study; in the collection, analyses, or interpretation of data; in the writing of the manuscript, or in the decision to publish the results.

References

1. Karnowsky, I. *Theory of Arched Structures*; Springer: Berlin/Heidelberg, Germany, 2012.
2. Stavridis, L. *Structural Systems: Behaviour and Design*; Thomas Telford: London, UK, 2010.
3. García-Guerrero, J.M. The Spatial Arch Bridge as a Typological Evolution (El Puente Arco Espacial Como una Evolución Tipológica). Ph.D. Thesis, Technical University of Cartagena, Cartagena, Spain, 2018. (In Spanish).
4. Jorquera-Lucerga, J.J. Form-finding of funicular geometries in spatial arch bridges through simplified force density method. *Appl. Sci.* **2018**, *8*, 2553. [CrossRef]
5. Thalla, O.; Stiros, S.C. Wind-induced fatigue and asymmetric damage in a timber bridge. *Sensors* **2018**, *18*, 3867. [CrossRef] [PubMed]
6. Gentile, R.; Nettis, A.; Raffaele, D. Effectiveness of the displacement-based seismic performance assessment for continuous RC bridges and proposed extensions. *Eng. Struct.* **2020**, *221*, 110910. [CrossRef]
7. Gou, H.; Zhou, W.; Yang, C.; Bao, Y.; Pu, Q. Dynamic response of a long-span concrete-filled steel tube tied arch bridge and the riding comfort of monorail trains. *Appl. Sci.* **2018**, *8*, 650. [CrossRef]

8. Manterola-Armisén, J. *Puentes (Bridge Engineering)*; Colegio de Ingenieros de Caminos, Canales y Puertos: Madrid, Spain, 2006; pp. 897–988; ISBN 9788438003220. (In Spanish)
9. Palkowski, S. Buckling of parabolic arches with hangers and tie. *Eng. Struct.* **2012**, *44*, 128–132. [CrossRef]
10. Tzonis, A. *Santiago Calatrava: Obra Completa*; Ediciones Polígrafa: Barcelona, Spain, 2007; ISBN 8434311518.
11. Jorquera-Lucerga, J.J. Understanding Calatrava's bridges: A conceptual approach to the 'La Devesa-type' footbridges. *Eng. Struct.* **2013**, *56*, 2083–2097. [CrossRef]
12. García-Guerrero, J.M.; Jorquera-Lucerga, J.J. Effect of stiff hangers on the longitudinal structural behavior of tied-arch bridges. *Appl. Sci.* **2018**, *8*, 258. [CrossRef]
13. García-Guerrero, J.M.; Jorquera-Lucerga, J.J. Influence of stiffened hangers on the structural behavior of all-steel tied-arch bridges. *Steel Compos. Struct.* **2019**, *32*, 479–495. [CrossRef]
14. Leonhardt, F. *Bridges, Brücken*; The Architectural Press: London, UK, 1982; pp. 38–43.
15. Lebet, J.P.; Hirt, M.A. *Steel Bridges*; EPFL Press: Lausanne, Switzerland, 2013; pp. 461–488; ISBN 9781466572973.
16. European Committee for Standardization (CEN). *Eurocode 3: Design of Steel Structures—Part 2: Steel Bridges*; CEN: Brussels, Belgium, 2006.
17. European Committee for Standardization (CEN). *Eurocode 1: Actions on Structures—Part 2: Traffic Loads on Bridges*; CEN: Brussels, Belgium, 2003.
18. Computers and Structures, Inc. *Analysis Reference Manual for SAP2000®v 16*; CSI: Berkeley, CA, USA, 2013.
19. Menn, C. *Prestressed Concrete Bridges*; Birkhäuser Verlag: Vienna, Austria, 1989; pp. 382–394. ISBN 9783034899208.
20. Jorquera-Lucerga, J.J. A Study on Structural Behaviour of Spatial Arch Bridges (Estudio del Comportamiento Resistente de los Puentes Arco Espaciales). Ph.D. Thesis, Technical University of Madrid, Madrid, Spain, 2007. (In Spanish).
21. Ortiz Berrocal, L. *Resistencia de Materiales*; McGraw-Hill: Madrid, Spain, 1990; pp. 81–99. ISBN 8476155123.
22. Oudin-Hograindleur, H.; Fontaine, J.-F.; Virlogeux, M. La passerelle de Montigny-lès-Cormeilles. *Bull. Ouvrages Métalliques* **2001**, *1*, 78–93.
23. Sacristán, M.; Capellán, G.; Merino, E.; Martínez, J. Architectural engineering applied to the design of urban bridges. New paradigms for the use of classic typologies in urban areas. In *Large Structures and Infrastructures for Environmentally Constrained and Urbanised Areas, Proceedings of the 34th IABSE Symposium, Venice, Italy, 22–24 September 2010*; IABSE: Zurich, Switzerland, 2010; Volume 97, pp. 25–32.
24. Arenas de Pablo, J.J.; Pantaleón, M.J. Barqueta Bridge, Sevilla, Spain. *Struct. Eng. Int.* **1992**, *2*, 251–252. [CrossRef]
25. Ministerio de Fomento. *Instrucción de Acero Estructural, (EAE)*; Ministerio de Fomento: Madrid, Spain, 2011.
26. The MathWorks Inc. *Matlab R2014*, 2014.